



Liquid–liquid phase separation in organic particles consisting of α -pinene and β -caryophyllene ozonolysis products and mixtures with commercially-available organic compounds

5 Young-Chul Song¹, Ariana G. Bé², Scot T. Martin³, Franz M. Geiger², Allan K. Bertram⁴, Regan J. Thomson², and Mijung Song^{1*}

¹Department of Earth and Environmental Sciences, Jeonbuk National University, Jeollabuk-do, Republic of Korea

²Department of Chemistry, Northwestern University, Evanston, Illinois 60208, United States

10 ³School of Engineering and Applied Sciences & Department of Earth and Planetary Sciences, Harvard University, Cambridge, Massachusetts 02138, United States

⁴Department of Chemistry, University of British Columbia, Vancouver, BC, V6T 1Z1, Canada

Correspondence: Mijung Song (mijung.song@jbnu.ac.kr)

15

Abstract

Liquid–liquid phase separation (LLPS) in organic aerosol particles can impact several properties of atmospheric particulate matter, such as cloud condensation nuclei (CCN) properties, optical properties, and gas-to-particle partitioning. Yet, our understanding of LLPS in organic aerosols is far from
20 complete. Here, we report on LLPS of one-component and two-component organic particles consisting of α -pinene- and β -caryophyllene-derived ozonolysis products and commercially-available organic compounds of relevance to atmospheric organic particles. In the experiments involving single-component organic particles, LLPS was observed in 8 out of 11 particle types studied. LLPS almost
25 always occurred when the oxygen-to-carbon elemental ratio (O:C) was ≤ 0.44 , but did not occur when O:C was > 0.44 . The phase separation occurred by spinodal decomposition, and when LLPS occurred, two liquid phases co-existed up to $\sim 100\%$ relative humidity (RH). In the experiments involving two-



component organic particles, LLPS was observed in 23 out of 25 particles types studied. LLPS almost always occurred when the average was $O:C \leq 0.67$, but never occurred when the average $O:C$ was > 0.67 . The phase separation occurred by spinodal decomposition or growth of a second phase at the surface of the particles. When LLPS occurred, two liquid phases co-existed up to $\sim 100\%$. These results provide further evidence that LLPS is likely a frequent occurrence in organic aerosol particles in the troposphere, even in the absence of inorganic salts.

1. Introduction

Secondary organic aerosols (SOA) are ubiquitous in the atmosphere, comprising up to approximately 80% of the mass of submicrometer particles (Kanakidou et al., 2005; Jimenez et al., 2009; Heald et al., 2010). SOA particles are produced when OH, NO_3 , and O_3 oxidize volatile organic compounds (VOC) in the atmosphere. Depending on the VOC type, oxidant type, and reaction time, the oxygen-to-carbon elemental ratio ($O:C$) of SOA can vary from 0.2 to 1.0 (Zhang et al., 2007; Hallquist et al., 2009; Jimenez et al., 2009; Heald et al., 2010; Ng et al., 2010). SOA particles are important because they play critical roles in air quality, cloud formation, and the Earth's radiative properties (Seaton et al., 1995; Xiaohong and Jian, 2010; Pöschl and Shiraiwa, 2015; Sanchez et al., 2017; Shiraiwa et al., 2017).

SOA can undergo phase transitions as relative humidity (RH) changes in the atmosphere (Hänel, 1976; Martin, 2000; Krieger et al., 2012; You et al., 2014; Freedman, 2017). One possible phase transition is liquid–liquid phase separation (LLPS) (Pankow, 2003; Marcolli and Krieger, 2006; Ciobanu et al., 2009; Bertram et al., 2011; Krieger et al., 2012; Song et al., 2012a; Zuend and Seinfeld, 2012; Veghte et al., 2014; You et al., 2014; O'Brien et al., 2015; Freedman, 2017). The occurrence of LLPS has implications for the optical properties (Brunamonti et al., 2015; Fard et al., 2018), gas-particle partitioning (Zuend et al., 2010; Zuend and Seinfeld, 2012; Shiraiwa et al., 2013), hygroscopic properties (Hodas et al., 2016), and cloud condensation nuclei (CCN) properties (Ovadnevaite et al., 2017; Liu et al. 2018) of atmospheric particles.

Many researchers have focused on LLPS in particles containing organic material mixed with inorganic salts. They found that LLPS can occur when the $O:C$ of the organic material is smaller than 0.8 (Bertram et al., 2011; Krieger et al., 2012; Song et al., 2012a, 2012b; Schill and Tolbert, 2013; You



55 et al., 2013, 2014). More recently, studies on LLPS in organic aerosol particles free of inorganic salts
have shown that LLPS occurs in SOA generated in environmental chambers when the average O:C of
the organic material is smaller than roughly 0.5 across the RH range of ~95% to ~100% (Renbaum-
Wolff et al., 2016; Rastak et al., 2017; Song et al., 2017; Ham et al., 2019) with implications for the
CCN properties of the SOA (Petters et al., 2006; Hodas et al., 2016; Renbaum-Wolff et al., 2016;
60 Ovadnevaite et al., 2017; Rastak et al., 2017; Liu et al., 2018; Ham et al., 2019). Consistent with these
laboratory studies, a recently introduced binary activity thermodynamic (BAT) model, with reduced
complexity for atmospheric modelling, predicts that LLPS can occur when the O:C of the organic
material is < 0.5 (Gorkowski et al., 2019), when considering different types of functional groups. In
addition, Song et al. (2018) showed that LLPS occurs in organic particles containing one commercially-
65 available organic compound when the O:C is smaller than 0.44 while LLPS occurs in organic particles
containing two commercially available organic species when the average the O:C is smaller than ≤ 0.58 .

In the following, we investigated LLPS in particles containing one and two organic species generated
from ozonolysis products of α -pinene and β -caryophyllene, which are atmospherically relevant, and
commercially-available organic compounds. These results provide additional insight into the O:C range
70 required for LLPS in organic particles free of inorganic salts.

2. Experimental

2.1 Materials

Table 1 presents the physical properties of the organic compounds investigated. In this study, 11 organic
75 species were used, including seven products from the ozonolysis of α -pinene and β -caryophyllene and
four commercially-available organic compounds. These species covered an O:C range of 0.13 - 1.00
(Table 1). All species were liquid at room temperature.

Seven of the products from the ozonolysis of α -pinene and β -caryophyllene were synthesized. The
detailed synthesis methods for these species are described in Bé et al. (2017). Using ^1H NMR, ^{13}C NMR,
80 and IR spectroscopy, the ozonolysis products were characterized to confirm their identity and purity.
All products contained a carboxylic acid, ketone, and/or aldehyde, which are abundant organic
functional groups in the atmosphere (Hallquist et al., 2009; Nozière et al., 2015). The O:C range of the



ozonolysis products was between 0.13 and 0.44 (Table 1). To achieve O:C ratios up to 1.00, we used commercially-available organic compounds (Sigma-Aldrich, purities $\geq 97\%$) (Table 1).

85

2.2 Preparation of particles consisting of one and two organic species

Particles consisting of either one or two organic compounds were prepared at room temperature without the addition of a solvent. Particles consisting of the commercially-available organic compounds were nebulized directly on siliconized hydrophobic glass slides (Hampton Research, Canada). Particles
90 consisting of ozonolysis products were slightly viscous. To form particles on a substrate, these ozonolysis products were picked up with the tip of a pipette, and the pipette was then flicked towards a hydrophobic glass slide.

Particles consisting of two organic compounds were prepared using mixtures (1:1 mass ratio) of pure organic species without addition of a solvent. To prepare the mixtures with 1:1 mass ratio, each organic
95 species was weighed in a vial and then combined. After mixing, the solutions were homogenous based on visual inspection. Particles were generated from these mixtures and deposited on hydrophobic slides either by nebulization (for the mixtures involving commercially-available organic compounds) or by the flicking method via the tip of a pipette as described above (for the ozonolysis products). This method of producing two-component organic particles did not work for α -pinene ozonolysis products and β -
100 caryophyllinic acid due to the stickiness of these material. Hence, these materials were not included in the systems used to generate two-component organic particles.

2.3 Optical microscopy for observation of liquid–liquid phase separation

The organic particles on hydrophobic glass slides were placed into a RH and temperature controlled
105 flow-cell coupled to an optical microscope (Olympus BX43, 40 \times objective, Japan) (Parsons et al., 2004; Pant et al., 2006; Bertram et al., 2011; Song et al., 2012a, 2018; Ham et al., 2019). During all experiments, the temperature inside the flow-cell was maintained at 291 ± 1 K. The RH was controlled by a continuous flow of a wet and dry N_2 mixture with a total flow rate of 500 sccm. The temperature and RH were monitored by a humidity and temperature sensor (Sensirion, SHT 71, Switzerland). RH
110 inside the flow-cell was calibrated by measuring the deliquescence RH of four different pure inorganic



salts (potassium carbonate, sodium chloride, ammonium sulfate, and potassium nitrate) (Winston and Bates, 1960). The RH uncertainty from the calibration was $\pm 1.5\%$.

At the beginning of LLPS experiments, organic particles inside the flow-cell were equilibrated at $\sim 100\%$ RH for 15–20 min. If LLPS was observed, the RH was decreased from $\sim 100\%$ to $\sim 5\text{--}10\%$ lower than the RH at which the two liquid phases merged into one phase followed by an increase in RH to $\sim 100\%$. If LLPS was not observed, the RH was decreased from $\sim 100\%$ to $\sim 0\%$ RH, followed by an increase to $\sim 100\%$ RH. During all experiments, the RH was adjusted at a rate of $0.1 - 0.2\%$ RH min^{-1} . The optical images during experiments were recorded every 5 s using a CMOS (complementary metal–oxide–semiconductor) detector (DigiRetina 16, Tucsen, China). Organic particles were selected in the diameter range of $30\text{--}100\ \mu\text{m}$, which was required for LLPS experiments.

3. Results and discussion

3.1 Liquid–liquid phase separation in particles containing one organic species

Eleven different types of particles containing one organic species were investigated for LLPS at 291 ± 1 K. Out of the eleven different types of one-component organic particles studied, eight underwent LLPS during humidity cycles (Table S1). LLPS occurred in all one-component organic particles containing α -pinene and β -caryophyllene ozonolysis products.

Shown in Figure 1 and Movies S1–S7 are optical images recorded while the RH was decreased for all the cases where LLPS was observed in one-component organic particles. For these cases, two liquid phases were always observed at $\sim 100\%$ RH. As the RH was decreased, the two liquid phases merged into one liquid phase at $\sim 95\%$ RH, except for particles of β -caryophyllinic acid (Fig. 1e and Movie S5). For β -caryophyllinic acid particles, the two liquid phases merged into one liquid phase at 83.7% RH (Fig. 1e and Movie S5). Particles of β -caryophyllonic acid and β -nocaryophyllonic acid had a partially engulfed morphology after LLPS (Fig. 1b, d and Movies S2, S4) (Kwamena et al., 2010; Reid et al., 2011; Song et al., 2013) while the others particles had a core-shell morphology after LLPS. We expect that the inner phase consisted mainly of water while the outer phase consisted mainly of organic molecules because the amount of the inner phase reduced in size as the RH was decreased (Renbaum-Wolff et al., 2016; Song et al., 2017, 2018).



Shown in Figure 2 and Movies S8-S14 are optical images of the same seven particles shown in Fig. 1
140 and Movies S1-S7, except the images were recorded while the RH was increased, rather than decreased.
At low RH-values, the particles contained one phase. As the RH increased, LLPS occur at ~95% RH for
all cases exception for β -caryophyllinic acid particles, which underwent LLPS at 84.9% RH (Fig. 2e
and Movie S12). At the onset of LLPS, many small inclusions formed in the particles. As the RH was
further increased, the small inclusions coagulated and coalesced, and the particles continued to grow
145 (Fig. 2 and Movies S8-S14). At ~100% RH, all particles contained two liquid phases.

The mechanism for LLPS in the single-component organic particles was likely spinodal
decomposition based on the formation of many small inclusions at the onset of LLPS. Spinodal
decomposition is a phase transition that occurs within a liquid without an energy barrier (Shelby, 1995;
Papon et al., 1999; Ciobanu et al., 2009; Song et al., 2012a). Previous studies also observed LLPS by
150 spinodal decomposition in α -pinene-derived SOA, β -caryophyllene-derived SOA, and limonene-derived
SOA (Renbaum-Wolff et al., 2016; Song et al., 2017; Ham et al., 2019).

Illustrated in Fig. 3a is the lower RH boundary for LLPS ($LLPS_{lower}$) and upper RH boundary for
LLPS ($LLPS_{upper}$) determined for one-component organic particles (blue symbols). LLPS occurred in
the one-component organic particles when the O:C was ≤ 0.44 . Our results are consistent with the
155 results from Song et al. (2018), who observed LLPS in one-component organic particles when the O:C
was ≤ 0.44 (Fig. 3a, grey symbols). Our results are also consistent with $LLPS_{lower}$ and $LLPS_{upper}$
determined for SOA produced from α -pinene and β -caryophyllene (Renbaum-Wolff et al., 2016; Song
et al., 2017; Ham et al., 2019). In all cases, $LLPS_{upper}$ was ~ 100% RH.

The values of $LLPS_{lower}$ and $LLPS_{upper}$ determine in the current experiments using a decreasing RH
160 was within the uncertainty of $LLPS_{lower}$ and $LLPS_{upper}$ values determine in the experiments using an
increasing RH (Tables S1 and S2). In addition, no dependence on particle size was observed for
 $LLPS_{lower}$ and $LLPS_{upper}$ within the size range investigated (30–100 μm).

Figure 4 shows the occurrence of LLPS in single-component organic particles as a function of O:C
and molar mass from the current study and as well as that of Song et al. (2018). For comparison
165 purposes, also included in Fig. 4 is the miscibility boundary of organic compounds based on the BAT
model (Gorkowski et al., 2019). Three of our measurements appear to disagree with the BAT model.



The small discrepancies between the current results and the predictions from the BAT model is likely related to the uncertainty in the BAT model (approximately an uncertainty of ± 0.03 O:C units) and difference in organic compounds used in the current study and used to generate the BAT model. In the current study, we investigated compounds with more than one type of functional group while the BAT model used a single type of functional group to generate miscibility boundaries.

3.2 Liquid-liquid phase separation in particles containing two organic species

To better mimic the complexity of real aerosol compositions, we also studied LLPS in particles containing two organic species. Table S2 lists the 25 different mixtures investigated using combinations of β -caryophyllene ozonolysis products and commercially-available organic compounds. In total, 23 out of the 25 two-component organic particle types investigated underwent LLPS (Fig. 3b and Table S2). Shown in Fig. 5 and Movies S15-S19 are examples of images of two-component organic particles that underwent LLPS during a decrease in RH. Shown in Fig. 6 and Movies S20-S24 are the same five particles, but images recorded as the RH was increased.

Out of the 23 particles types that underwent LLPS, 19 of the particle types formed a core-shell morphology with decreasing RH. Only four particle types (β -caryophyllonic acid/suberic acid, β -caryophyllonic acid/polyethylene glycol-400(PEG-400), β -caryophyllene aldehyde/ β -caryophyllonic acid, and β -caryophyllonic acid/ β -nocaryophyllonic acid) formed a partially engulfed morphology with decreasing RH. As discussed in Sect. 3.1, the inner phase is expected to be mainly water while the outer phase is expected to be mainly organic material (Renbaum-Wolff et al., 2016; Song et al., 2017, 2018). As RH was decreased, the two liquid phases merged into one phase. For example, particles of β -caryophyllene aldehyde/PEG-400 merged into one phase at 39.9% RH (Fig. 5e and Movie S19).

In the experiments with two-component organic particles and increasing RH, in most cases (19 out of the 23 particle types that underwent LLPS), phase separation began with the abrupt formation of many small inclusions (e.g. Fig. 6a, b, e and Movies S20, 21, 24). This behavior suggests spinodal decomposition as the mechanism for LLPS. In contrast, in experiments with particles containing ozonolysis products mixed with pyruvic acid, phase separation began with the growth of a second phase at the surface of the particle as the RH increased (Figs. 6c, d and Movies S22, 23). This type of



195 mechanism was previously observed in organic/inorganic aerosol particles (Ciobanu et al., 2009; Song et al., 2012a).

Illustrated in Fig. 3b (blue symbols) is the lower RH boundary for LLPS ($LLPS_{lower}$) and upper RH boundary for LLPS ($LLPS_{upper}$) determined in the experiments with two-component organic particles. LLPS was observed in all cases when the average O:C ≤ 0.67 . When LLPS was observed, $LLPS_{upper}$ was
200 $\sim 100\%$ RH. These results are similar to previous results from Song et al. (2018) (gray symbols in Fig. 3b), even though they studied different types of two-component organic particles. Figure 3b also presents Sigmoid-Boltzmann fits of all data points from Song et al. (2018) and the current study to parameterize $LLPS_{lower}$ (solid line) and $LLPS_{upper}$ (dashed line) as a function of O:C. The parametrizations of Sigmoid-Boltzmann fits are given in the Supplement Information (Sect. S2).

205

4. Atmospheric implications

O:C of organic materials has been used to interpret and parameterize hygroscopicity (Jimenez et al., 2009), oxidation (Heald et al., 2010; Kroll et al., 2011), and mixing thermodynamics of organic aerosol particles (Donahue et al., 2011; Hodas et al., 2016). Previous studies have shown LLPS in mixed
210 organic and inorganic aerosol particles often occurs for O:C < 0.8 (Bertram et al., 2011; Krieger et al., 2012; Song et al., 2012a, 2012b; Schill and Tolbert, 2013; You et al., 2013, 2014). Even in the absence of inorganic salts, the occurrence of LLPS was dependent on the O:C of organic materials (Renbaum-Wolff et al., 2016; Song et al., 2017; Song et al., 2018; Ham et al., 2019). Our results show that as compositional complexity increased from one organic species to two organic species, LLPS occurred
215 over a wider range of average O:C values of organic materials (increasing from 0.44 to 0.67) (Figs. 3a and b). Considering the chemical complexity and the O:C ratio of organic particles in the troposphere ($0.20 < O:C < 1.00$) (Zhang et al., 2007; Hallquist et al., 2009; Jimenez et al., 2009; Heald et al., 2010; Ng et al., 2010), our result provided additional evidence that LLPS is likely a common feature of organic aerosols free of inorganic salts. A caveat is that the mixing ratio of 1:1 for two organic species
220 and the chemical complexity used in our experiments is rather simple compared to the chemical complexity found in the atmosphere (Zhang et al., 2007; Hallquist et al., 2009; Jimenez et al., 2009).



Further studies are needed to confirm LLPS in organic aerosols comprising of more complex mixtures with different mixing ratios.

The occurrence of LLPS in organic aerosol particles at high RH, as observed in the current studies, is important since LLPS at high RH can lower the barrier to CCN activation by decreasing the surface tension of the particles (Ovadnevaite et al., 2017; Rastak et al., 2017; Liu et al., 2018). A decrease in surface tension and lowering of the barrier to CCN, can lead to an increase in cloud droplets numbers in the atmosphere, with implications for modelling the indirect effect of aerosols on climate (Ovadnevaite et al., 2017; Rastak et al., 2017).

230

Data availability. Underlying material and related items for this paper are located in the Supplement.

Author contributions. MS, AKB, and RJT designed the study. YS and MS conducted LLPS experiments and analyzed the data. AGB, FMG, and RJT produced ozonolysis products. YS and MS prepared the manuscript with contributions from AGB, STM, FMG, AKB, and RJT.

235

Competing interests. The authors declare that they have no conflict of interest.

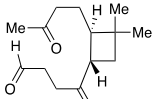
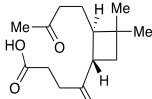
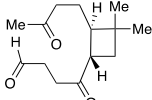
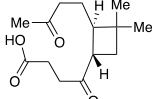
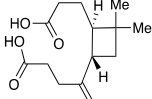
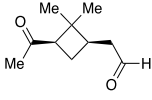
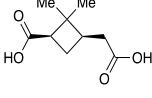
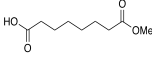
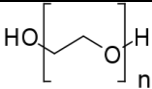
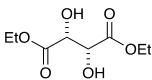
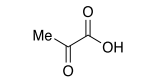
Acknowledgements. For authors at Jeonbuk National University, this work was supported by the National Research Foundation of Korea grant funded by the Korea Government (2019R1A2C1086187) and by Research Base Construction Fund Support Program funded from Jeonbuk National University in 2020. M. Song gives thanks to G. Jo for the technical support. The US National Science Foundation (AGS-1640378) is acknowledged by authors from Harvard University. The authors at Northwestern University acknowledge support from the US National Science Foundation (CHE-1607640 and Graduate Research Fellowship to AGB).

245



250 temperature.

Table 1. Molecular formula, molecular structure, molecular weight, oxygen-to-carbon elemental ratios (O:C), and functional groups of organic compounds studied. All compounds are liquid at room

Compounds		Molecular formula	Molecular structure	Molecular weight (g/mol)	O: C	Functional group
Ozonolysis products	β -caryophyllene aldehyde	$C_{15}H_{24}O_2$		237.19	0.13	Aldehyde, Ketone
	β -caryophyllonic acid	$C_{15}H_{24}O_3$		252.35	0.20	Carboxylic acid, Ketone
	β -nocaryophyllone aldehyde	$C_{14}H_{22}O_3$		238.32	0.21	Aldehyde, Ketone
	β -nocaryophyllonic acid	$C_{14}H_{22}O_4$		254.32	0.29	Carboxylic acid, Ketone
	β -caryophyllinic acid	$C_{14}H_{22}O_4$		254	0.29	Carboxylic acid
	Pinonaldehyde	$C_{10}H_{16}O_2$		169.12	0.20	Aldehyde, Ketone
	Pinic acid	$C_9H_{14}O_4$		209.08	0.44	Carboxylic acid, Ketone
Commercially-available organic compounds	Suberic acid monomethyl ester	$C_9H_{16}O_4$		188	0.44	Carboxylic acid, Ester
	Polyethylene glycol-400	$C_{2n}H_{4n+2}O_{n+1}$		400	0.56	Alcohol, Ether
	Diethyl L-tartrate	$C_8H_{14}O_6$		206	0.75	Alcohol, Ester
	Pyruvic acid	$C_3H_4O_3$		88.06	1.00	Carboxylic acid, Ketone

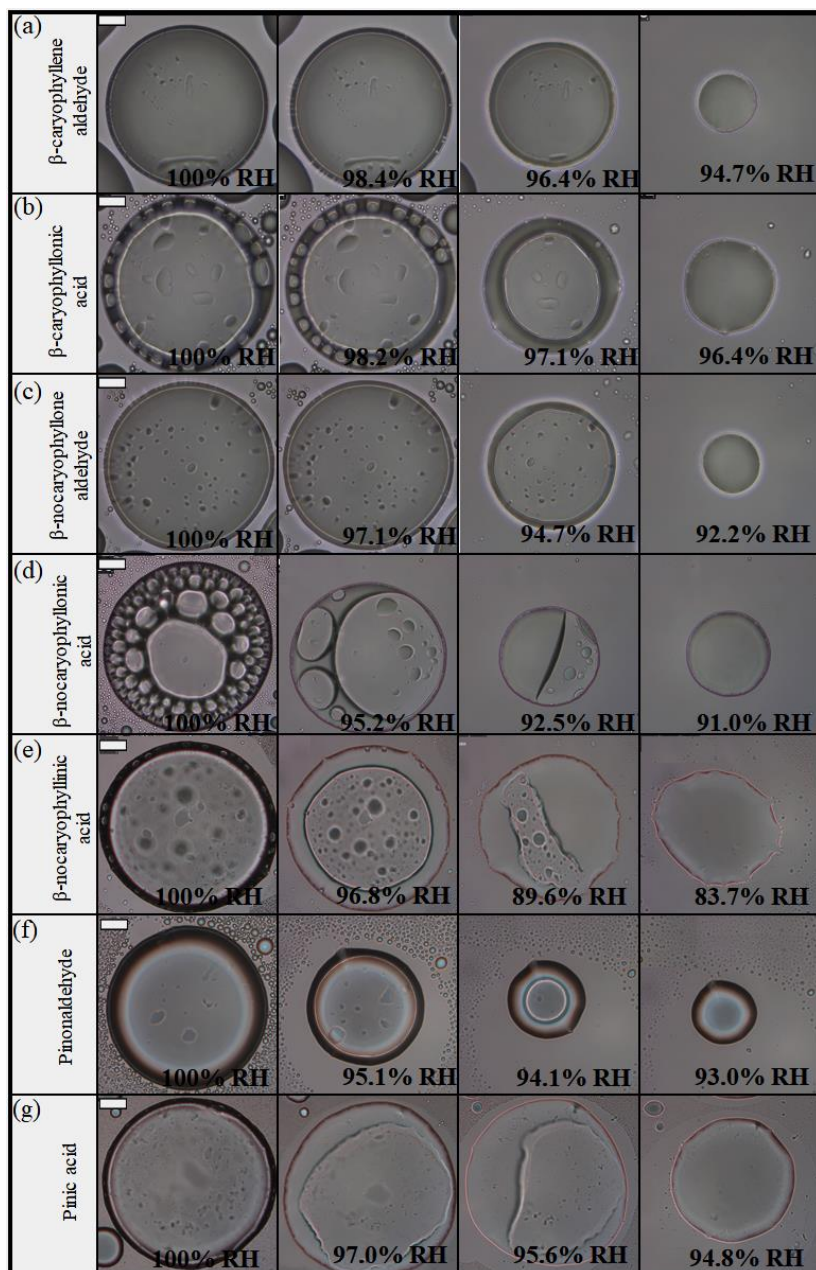


Figure 1. Optical images of particles for decreasing RH: (a) β -caryophyllene aldehyde, (b) β -caryophyllonic acid, (c) β -nocaryophyllone aldehyde, (d) β -nocaryophyllonic acid, (e) β -nocaryophyllinic acid, (f) pinonaldehyde, and (g) pinic acid. The last columns indicate the lower RH boundary for LLPS (LLPS_{lower}) with decreasing RH. The scale bar is 20 μ m.

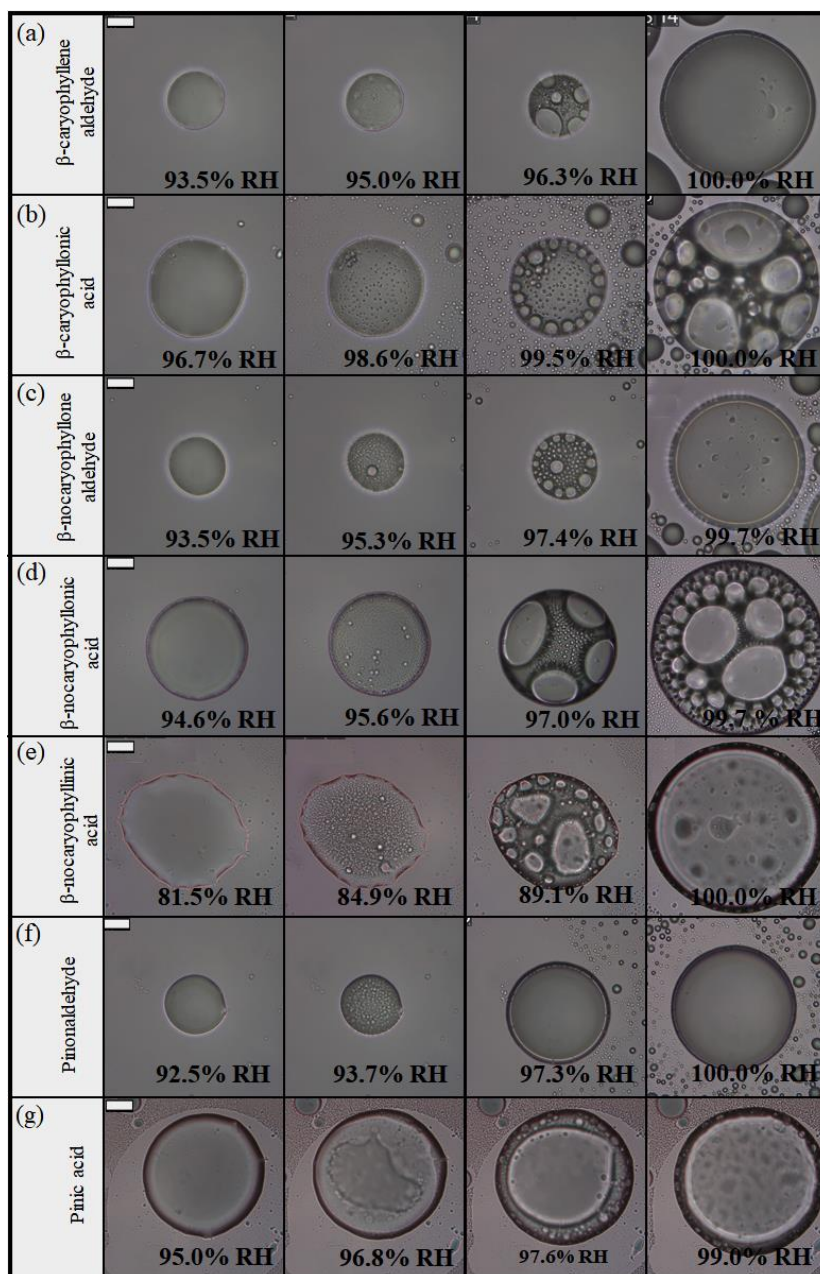


Figure 2. Optical images of particles for increasing RH: (a) β -caryophyllene aldehyde, (b) β -caryophyllonic acid, (c) β -nocaryophyllone aldehyde, (d) β -nocaryophyllonic acid, (e) β -nocaryophyllinic acid, (f) pinonaldehyde, and (g) pinic acid. The particles are the same ones in Fig. 1. The last columns indicate the upper RH boundary for LLPS ($\text{LLPS}_{\text{upper}}$) with increasing RH. The scale bar is 20 μm .

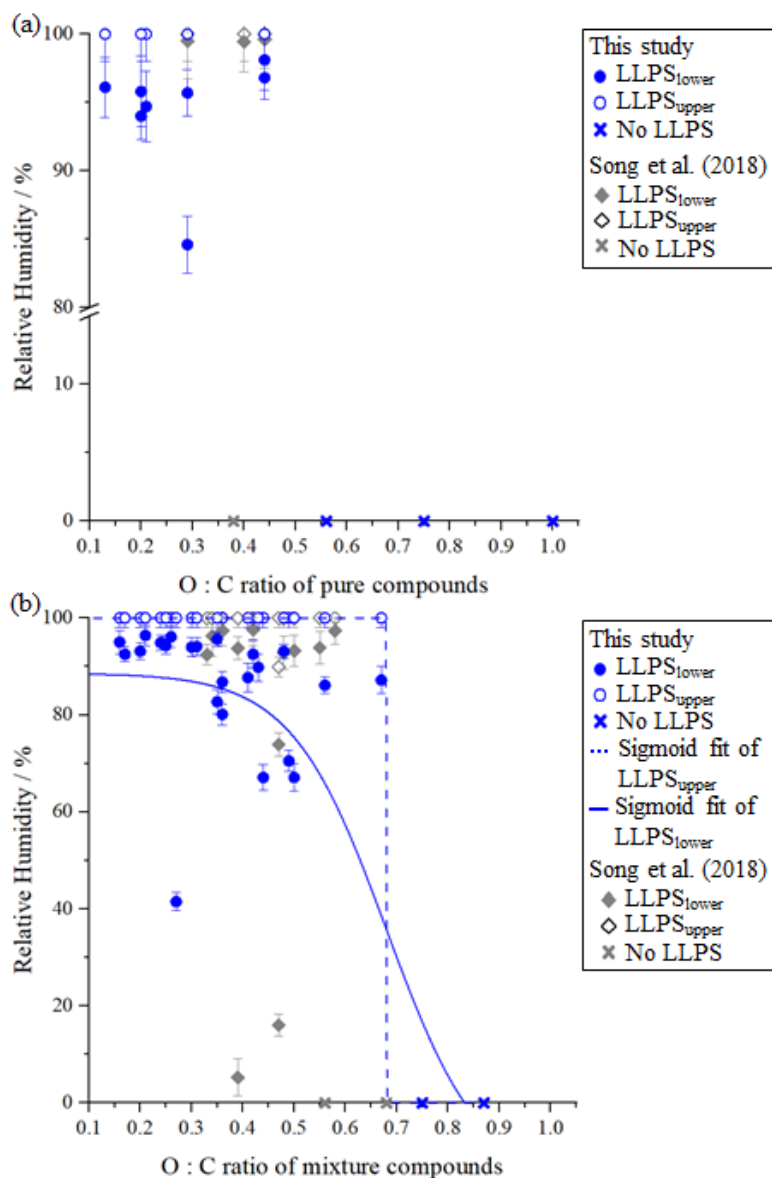
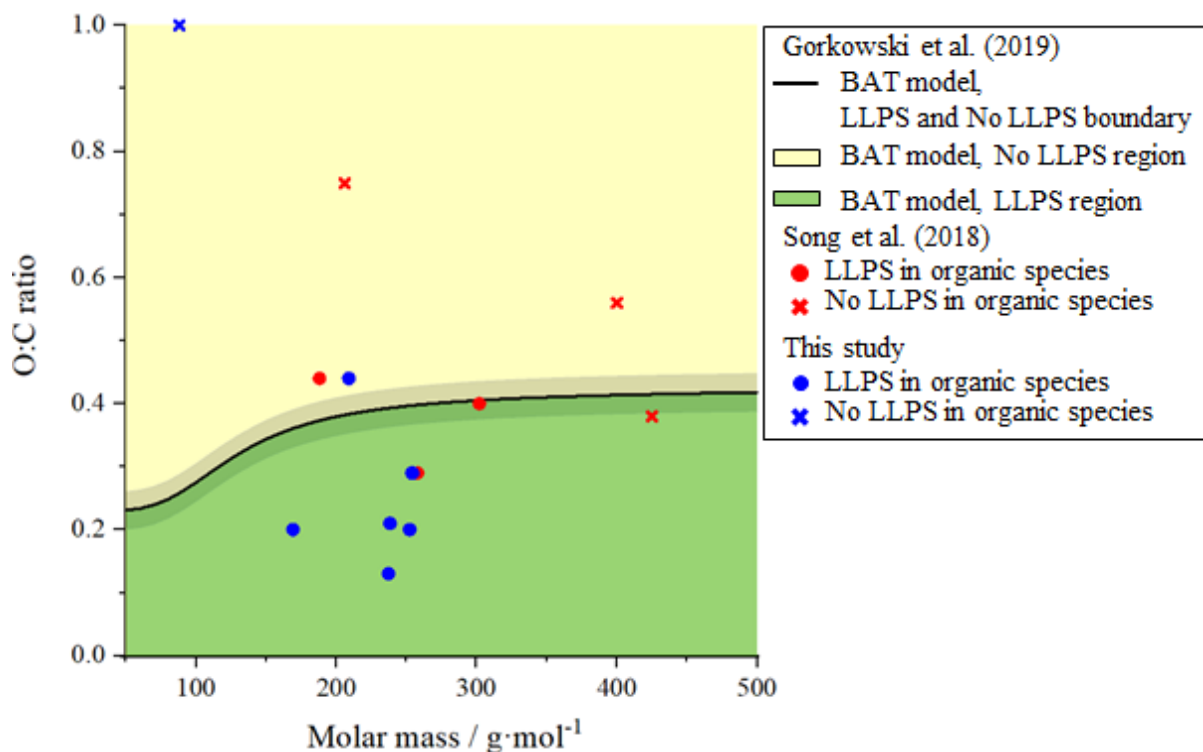


Figure 3. Relative humidity (RH) for LLPS as a function of the O:C of the organic particle consisting of:
(a) one organic species, and (b) two organic species for increasing RH. Open blue circles are the LLPS
265 upper boundary (LLPS_{upper}) with increasing RH, and closed blue circles are the LLPS lower boundary
(LLPS_{lower}) with increasing RH. The grey diamonds are the result from Song et al. (2018). Error bars
represent 2 σ of multiple measurements and the uncertainty from the RH calibration. The solid and
dashed lines are Sigmoid-Boltzmann fits to all the data of LLPS_{lower} and LLPS_{upper}.



270 Figure 4. LLPS as a function of O:C and molar mass of particles of one organic species. Green and
yellow regions indicate LLPS and no LLPS, respectively, in particles of one organic species using
binary activity thermodynamics (BAT) model from Gorkowski et al. (2019). Black line indicates
boundary of LLPS and no LLPS in the particles, and light gray shadow is the error region of the binary
activity thermodynamic (BAT) model. Circles and crosses indicate measured LLPS and no LLPS,
275 respectively, in one-component organic particles from Song et al. (2018) (red) and this study (blue).

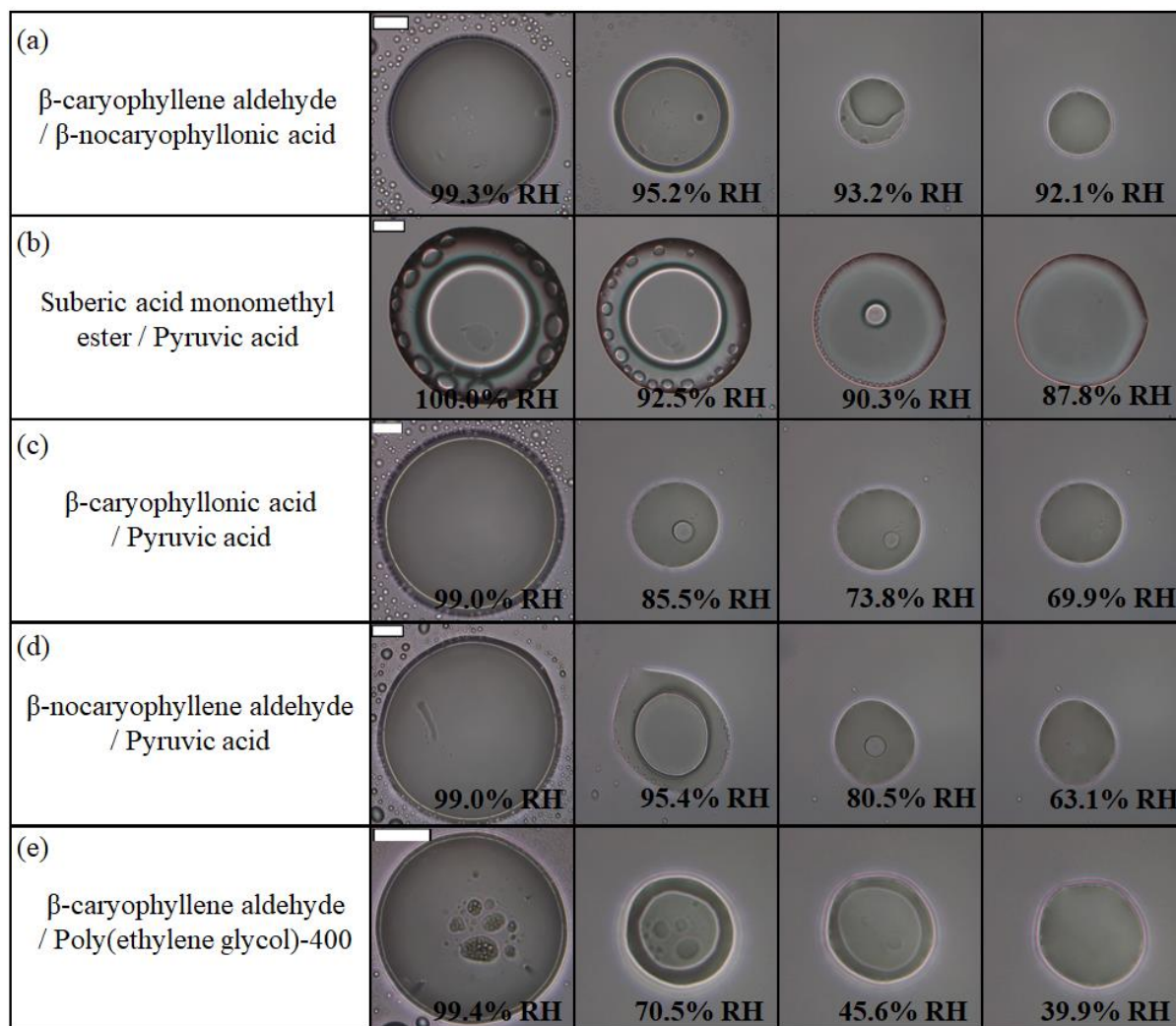
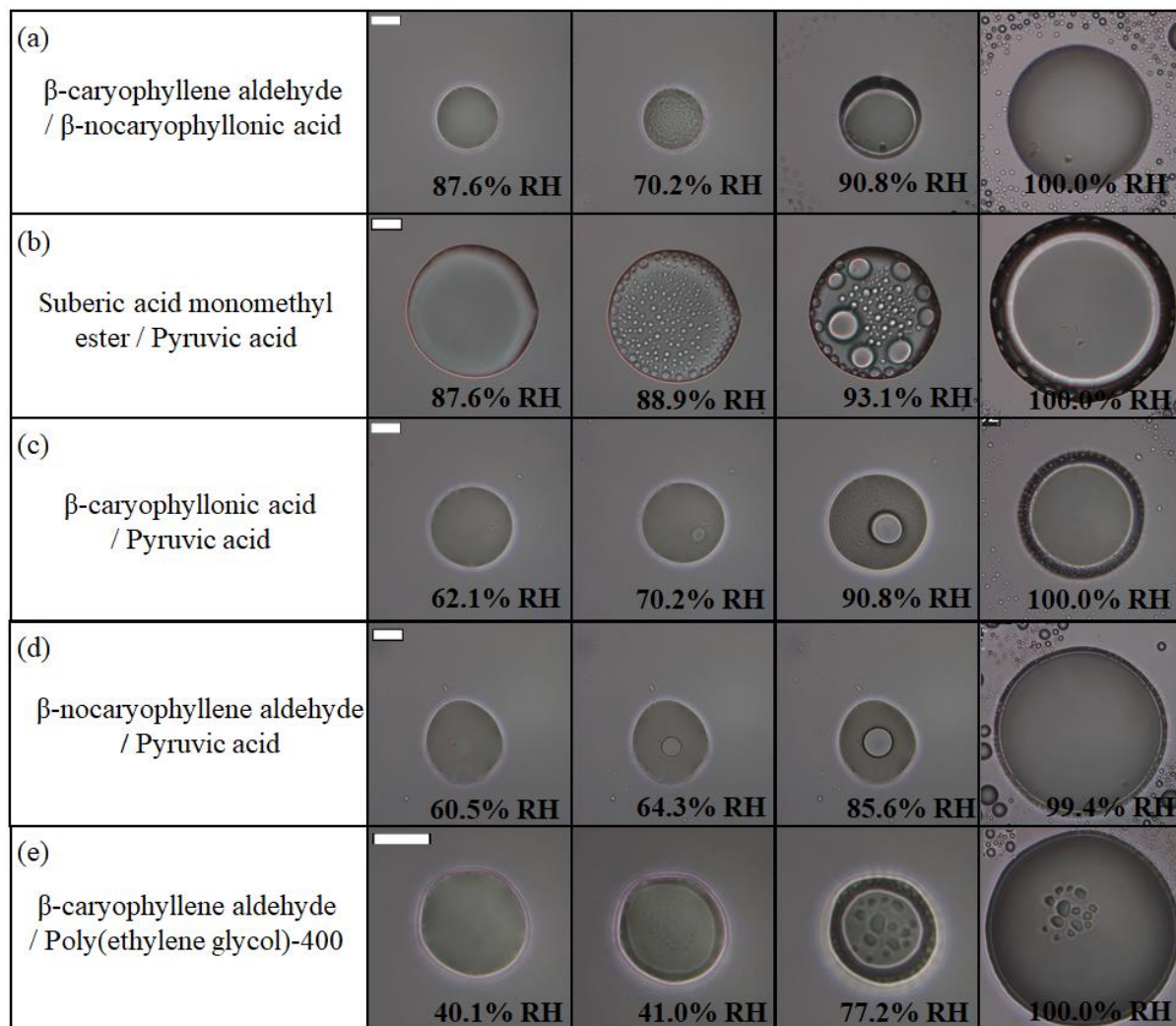


Figure 5. Optical images of two-component particles for decreasing RH: (a) β -caryophyllene aldehyde/ β -nocaryophyllonic acid, (b) Suberic acid monomethyl ester/pyruvic acid, (c) β -caryophyllonic acid/pyruvic acid, (d) β -nocaryophyllene aldehyde/pyruvic acid, and (e) β -caryophyllene aldehyde/polyethylene glycol-400. The last columns indicate the lower RH boundary for LLPS (LLPS_{lower}) with decreasing RH. The scale bar is 20 μ m.



285 Figure 6. Optical images of two-component particles for increasing RH: (a) β -caryophyllene aldehyde/ β -nocaryophyllonic acid, (b) Suberic acid monomethyl ester/pyruvic acid, (c) β -caryophyllonic acid/pyruvic acid, (d) β -nocaryophyllene aldehyde/pyruvic acid, and (e) β -caryophyllene aldehyde/polyethylene glycol-400. The particles are the same ones in Fig. 5. The last columns indicate the upper RH boundary for LLPS (LLPS_{upper}) with increasing RH. The scale bar is 20 μ m.



290 Reference

- Bé, A. G., Upshur, M. A., Liu, P., Martin, S. T., Geiger, F. M. and Thomson, R. J.: Cloud activation potentials for atmospheric α -pinene and β -caryophyllene ozonolysis products, *ACS Cent. Sci.*, 3(7), 715–725, doi:10.1021/acscentsci.7b00112, 2017.
- Bertram, A. K., Martin, S. T., Hanna, S. J., Smith, M. L., Bodsworth, A., Chen, Q., Kuwata, M., Liu, A.,
295 You, Y. and Zorn, S. R.: Predicting the relative humidities of liquid-liquid phase separation, efflorescence, and deliquescence of mixed particles of ammonium sulfate, organic material, and water using the organic-to-sulfate mass ratio of the particle and the oxygen-to-carbon ele, *Atmos. Chem. Phys.*, 11, 10995–11006, doi:10.5194/acp-11-10995-2011, 2011.
- Brunamonti, S., Krieger, U. K., Marcolli, C. and Peter, T.: Redistribution of black carbon in aerosol
300 particles undergoing liquid-liquid phase separation, *Geophys. Res. Lett.*, 42(7), 2532–2539, doi:10.1002/2014GL062908, 2015.
- Ciobanu, V. G., Marcolli, C., Krieger, U. K., Weers, U. and Peter, T.: Liquid-liquid phase separation in mixed organic/inorganic aerosol particles, *J. Phys. Chem. A*, 113(41), 10966–10978, doi:10.1021/jp905054d, 2009.
- 305 Donahue, N. M., Epstein, S. A., Pandis, S. N. and Robinson, A. L.: A two-dimensional volatility basis set: 1. Organic-aerosol mixing thermodynamics, *Atmos. Chem. Phys.*, 11(7), 3303–3318, doi:10.5194/acp-11-3303-2011, 2011.
- Fard, M. M., Krieger, U. K. and Peter, T.: Shortwave radiative impact of liquid-liquid phase separation in brown carbon aerosols, *Atmos. Chem. Phys.*, 18, 13511–13530, doi:10.5194/acp-18-13511-2018,
310 2018.
- Freedman, M. A.: Phase separation in organic aerosol, *Chem. Soc. Rev.*, 46, 7694–7705, doi:10.1039/C6CS00783J, 2017.
- Gorkowski, K., Preston, T. C. and Zuend, A.: RH-humidity-dependent organic aerosol thermodynamics via an efficient reduced-complexity model, *Atmos. Chem. Phys.*, 19, 13383–13407, doi:10.5194/acp-
315 2019-495, 2019.
- Hallquist, M., Wenger, J. C., Baltensperger, U., Rudich, Y., Simpson, D., Claeys, M., Dommen, J., Donahue, N. M., George, C., Goldstein, a. H., Hamilton, J. F., Herrmann, H., Hoffmann, T., Iinuma, Y.,



- Jang, M., Jenkin, M. E., Jimenez, J. L., Kiendler-Scharr, a., Maenhaut, W., McFiggans, G., Mentel, T. F., Monod, a., Prévôt, a. S. H., Seinfeld, J. H., Surratt, J. D., Szmigielski, R. and Wildt, J.: The
320 formation, properties and impact of secondary organic aerosol: current and emerging issues, *Atmos. Chem. Phys.*, 9(14), 5155–5236, doi:10.5194/acp-9-5155-2009, 2009.
- Ham, S., Babar, Z. Bin, Lee, J., Lim, H. and Song, M.: Liquid-liquid phase separation in secondary organic aerosol particles produced from α -pinene ozonolysis and α -pinene photo-oxidation with/without ammonia, *Atmos. Chem. Phys.*, 19(14), 9321–9331, doi:10.5194/acp-2019-19, 2019.
- 325 Hänel, G.: The single-scattering albedo of atmospheric aerosol particles as a function of relative humidity, *J. Atmos. Sci.*, 33(6), 1120–1124, doi:10.1175/1520-0469(1976)033<1120:tssaoa>2.0.co;2, 1976.
- Heald, C. L., Ridley, D. A., Kreidenweis, S. M. and Drury, E. E.: Satellite observations cap the atmospheric organic aerosol budget, *Geophys. Res. Lett.*, 37(24), 1–5, doi:10.1029/2010GL045095,
330 2010.
- Hodas, N., Zuend, A., Schilling, K., Berkemeier, T., Shiraiwa, M., Flagan, R. C. and Seinfeld, J. H.: Discontinuities in hygroscopic growth below and above water saturation for laboratory surrogates of oligomers in organic atmospheric aerosols, *Atmos. Chem. Phys.*, 16, 12767–12792, doi:10.5194/acp-16-12767-2016, 2016.
- 335 Jimenez, J. L., Canagaratna, M. R., Donahue, N. M., Prevot, a. S. H., Zhang, Q., Kroll, J. H., DeCarlo, P. F., Allan, J. D., Coe, H., Ng, N. L., Aiken, a. C., Docherty, K. S., Ulbrich, I. M., Grieshop, A. P., Robinson, a. L., Duplissy, J., Smith, J. D., Wilson, K. R., Lanz, V. a., Hueglin, C., Sun, Y. L., Tian, J., Laaksonen, A., Raatikainen, T., Rautiainen, J., Vaattovaara, P., Ehn, M., Kulmala, M., Tomlinson, J. M., Collins, D. R., Cubison, M. J., Dunlea, J., Huffman, J. A., Onasch, T. B., Alfarra, M. R., Williams, P. I.,
340 Bower, K., Kondo, Y., Schneider, J., Drewnick, F., Borrmann, S., Weimer, S., Demerjian, K., Salcedo, D., Cottrell, L., Griffin, R., Takami, a., Miyoshi, T., Hatakeyama, S., Shimono, A., Sun, J. Y., Zhang, Y. M., Dzepina, K., Kimmel, J. R., Sueper, D., Jayne, J. T., Herndon, S. C., Trimborn, a. M., Williams, L. R., Wood, E. C., Middlebrook, A. M., Kolb, C. E., Baltensperger, U., Worsnop, D. R., Dunlea, E. J., Huffman, J. A., Onasch, T. B., Alfarra, M. R., Williams, P. I., Bower, K., Kondo, Y., Schneider, J.,
345 Drewnick, F., Borrmann, S., Weimer, S., Demerjian, K., Salcedo, D., Cottrell, L., Griffin, R., Takami,



- a., Miyoshi, T., Hatakeyama, S., Shimono, A., Sun, J. Y., Zhang, Y. M., Dzepina, K., Kimmel, J. R., Sueper, D., Jayne, J. T., Herndon, S. C., Trimborn, a. M., Williams, L. R., Wood, E. C., Middlebrook, A. M., Kolb, C. E., Baltensperger, U., Worsnop, D. R., Dunlea, J., Huffman, J. A., et al.: Evolution of organic aerosols in the atmosphere, *Science* (80), 326(5959), 1525–1529, doi:10.1126/science.1180353, 350 2009.
- Kanakidou, M., Seinfeld, J. H., Pandis, S. N., Barnes, I., Dentener, F. J., Facchini, M. C., Van Dingenen, R., Ervens, B., Nenes, A., Nielsen, C. J., Swietlicki, E., Putaud, J. P., Balkanski, Y., Fuzzi, S., Horth, J., Moortgat, G. K., Winterhalter, R., Myhre, C. E. L., Tsigaridis, K., Vignati, E., Stephanou, E. G. and Wilson, J.: Organic aerosol and global climate modelling: a review, *Atmos. Chem. Phys.*, 5(4), 1053–355 1123, doi:10.5194/acp-5-1053-2005, 2005.
- Krieger, U. K., Marcolli, C. and Reid, J. P.: Exploring the complexity of aerosol particle properties and processes using single particle techniques., *Chem. Soc. Rev.*, 41(19), 6631–6662, doi:10.1039/c2cs35082c, 2012.
- Kroll, J. H., Donahue, N. M., Jimenez, J. L., Kessler, S. H., Canagaratna, M. R., Wilson, K. R., Altieri, 360 K. E., Mazzoleni, L. R., Wozniak, A. S., Bluhm, H., Mysak, E. R., Smith, J. D., Kolb, C. E. and Worsnop, D. R.: Carbon oxidation state as a metric for describing the chemistry of atmospheric organic aerosol., *Nat. Chem.*, 3(2), 133–139, doi:10.1038/nchem.948, 2011.
- Kwamena, N. O. A., Buajarn, J., and Reid, J. P.: Equilibrium morphology of mixed organic/inorganic/aqueous aerosol droplets: Investigating the effect of relative humidity and surfactants, 365 *J. Phys. Chem. A.*, 114, 5787–5795, doi:10.1021/Jp1003648, 2010.
- Liu, P., Song, M., Zhao, T., Gunthe, S. S., Ham, S., He, Y., Qin, Y. M., Gong, Z., Amorim, J. C., Bertram, A. K. and Martin, S. T.: Resolving the mechanisms of hygroscopic growth and cloud condensation nuclei activity for organic particulate matter, *Nat. Commun.*, doi:10.1038/s41467-018-06622-2, 2018.
- 370 Marcolli, C. and Krieger, U. K.: Phase changes during hygroscopic cycles of mixed organic/inorganic model systems of tropospheric aerosols, *J. Phys. Chem. A*, 110(5), 1881–1893, doi:10.1021/jp0556759, 2006.



- Martin, S. T.: Phase transitions of aqueous atmospheric particles, *Chem. Rev.*, 100(9), 3403–3453, doi:10.1021/cr990034t, 2000.
- 375 Ng, N. L., Canagaratna, M. R., Zhang, Q., Jimenez, J. L., Tian, J., Ulbrich, I. M., Kroll, J. H., Docherty, K. S., Chhabra, P. S., Bahreini, R., Murphy, S. M., Seinfeld, J. H., Hildebrandt, L., Donahue, N. M., Decarlo, P. F., Lanz, V. A., Prévôt, A. S. H., Dinar, E., Rudich, Y. and Worsnop, D. R.: Organic aerosol components observed in northern hemispheric datasets from aerosol mass spectrometry, *Atmos. Chem. Phys.*, 10(10), 4625–4641, doi:10.5194/acp-10-4625-2010, 2010.
- 380 Nozière, B., Kalberer, M., Claeys, M., Allan, J., D’Anna, B., Decesari, S., Finessi, E., Glasius, M., Grgić, I., Hamilton, J. F., Hoffmann, T., Iinuma, Y., Jaoui, M., Kahnt, A., Kampf, C. J., Kourchev, I., Maenhaut, W., Marsden, N., Saarikoski, S., Schnelle-Kreis, J., Surratt, J. D., Szidat, S., Szmigielski, R. and Wisthaler, A.: The molecular identification of organic compounds in the atmosphere: state of the art and challenges, *Chem. Rev.*, 115(10), 3919–3983, doi:10.1021/cr5003485, 2015.
- 385 O'Brien, R. E., Wang, B., Kelly, S. T., Lundt, N., You, Y., Bertram, A. K., Leone, S. R., Laskin, A. and Gilles, M. K.: Liquid-liquid phase separation in aerosol particles: Imaging at the nanometer scale, *Environ. Sci. Technol.*, 49(8), 4995–5002, doi:10.1021/acs.est.5b00062, 2015.
- Ovadnevaite, J., Zuend, A., Laaksonen, A., Sanchez, K. J., Roberts, G., Ceburnis, D., Decesari, S., Rinaldi, M., Hodas, N., Facchini, M. C., Seinfeld, J. H. and O’ Dowd, C.: Surface tension prevails over
390 solute effect in organic-influenced cloud droplet activation, *Nature*, 546(7660), 637–641, doi:10.1038/nature22806, 2017.
- Pankow, J. F.: Gas/particle partitioning of neutral and ionizing compounds to single and multi-phase aerosol particles. 1. Unified modeling framework, *Atmos. Environ.*, 37(24), 3323–3333, doi:10.1016/S1352-2310(03)00346-7, 2003.
- 395 Pant, A., Parsons, M. T. and Bertram, A. K.: Crystallization of aqueous ammonium sulfate particles internally mixed with soot and kaolinite: crystallization relative humidities and nucleation rates, *J. Phys. Chem. A*, 110(28), 8701–8709, doi:10.1021/jp060985s, 2006.
- Papon, P.; Leblond, J.; Meijer, P. H. E. *The Physics of Phase Transitions: Concepts and Applications*, Springer, 1999.



- 400 Parsons, M. T., Mak, J., Lipetz, S. R. and Bertram, A. K.: Deliquescence of malonic, succinic, glutaric, and adipic acid particles, *J. Geophys. Res. D Atmos.*, 109(6), 1–8, doi:10.1029/2003JD004075, 2004.
- Petters, M. D., Kreidenweis, S. M., Snider, J. R., Koehler, K. A., Wang, Q., Prenni, A. J. and Demott, P. J.: Cloud droplet activation of polymerized organic aerosol, *Tellus, Ser. B Chem. Phys. Meteorol.*, 58(3), 196–205, doi:10.1111/j.1600-0889.2006.00181.x, 2006.
- 405 Pöschl, U. and Shiraiwa, M.: Multiphase chemistry at the atmosphere–biosphere interface influencing climate and public health in the anthropocene, *Chem. Rev.*, 115(10), 4440–4475, doi:10.1021/cr500487s, 2015.
- Rastak, N., Pajunoja, A., Acosta Navarro, J. C., Ma, J., Song, M., Partridge, D. G., Kirkevåg, A., Leong, Y., Hu, W. W., Taylor, N. F., Lambe, A., Cerully, K., Bougiatioti, A., Liu, P., Krejci, R., Petäjä, T.,
- 410 Percival, C., Davidovits, P., Worsnop, D. R., Ekman, A. M. L., Nenes, A., Martin, S., Jimenez, J. L., Collins, D. R., Topping, D. O., Bertram, A. K., Zuend, A., Virtanen, A. and Riipinen, I.: Microphysical explanation of the RH-dependent water affinity of biogenic organic aerosol and its importance for climate, *Geophys. Res. Lett.*, 44(10), 5167–5177, doi:10.1002/2017GL073056, 2017.
- Reid, J. P., Dennis-Smith, B. J., Kwamena, N.-O. A., Miles, R. E. H., Hanford, K. L., and Homer, C.
- 415 J.: The morphology of aerosol particles consisting of hydrophobic and hydrophilic phases: hydrocarbons, alcohols and fatty acids as the hydrophobic component, *Phys. Chem. Chem. Phys.*, 13, 15559–15572, doi:10.1039/C1CP21510H,doi:10.1039/C1CP21510H, 2011.
- Renbaum-Wolff, L., Song, M., Marcolli, C., Zhang, Y., Liu, P. F., Grayson, J. W., Geiger, F. M., Martin, S. T. and Bertram, A. K.: Observations and implications of liquid-liquid phase separation at
- 420 high relative humidities in secondary organic material produced by α -pinene ozonolysis without inorganic salts, *Atmos. Chem. Phys.*, 16(12), 7969–7979, doi:10.5194/acp-16-7969-2016, 2016.
- Sanchez, K. J., Roberts, G. C., Calmer, R., Nicoll, K., Hashimshoni, E., Rosenfeld, D., Ovadnevaite, J., Preissler, J., Ceburnis, D., O’Dowd, C. and Russell, L. M.: Top-down and bottom-up aerosol-cloud-closure: towards understanding sources of uncertainty in deriving cloud radiative flux, *Atmos. Chem.*
- 425 *Phys.*, 17, 9797–9814, doi:doi.org/10.5194/acp-17-9797-2017, 2017.



- Schill, G. P. and Tolbert, M. A.: Heterogeneous ice nucleation on phase-separated organic-sulfate particles: effect of liquid vs. glassy coatings, *Atmos. Chem. Phys.*, 13(9), 4681–4695, doi:10.5194/acp-13-4681-2013, 2013.
- Seaton, A., MacNee, W., Donaldson, K. and Godden, D.: Particulate air pollution and acute health effects., *Lancet*, 345(8943), 176–178, doi:10.1016/S0140-6736(95)90173-6, 1995.
- Shelby, J. E. *Introduction to Glass Science and Technology*; The Royal Society of Chemistry: Cambridge, U.K., 1997
- Shiraiwa, M., Zuend, A. A., Bertram, A. K. and Seinfeld, J. H.: Gas-particle partitioning of atmospheric aerosols: interplay of physical state, non-ideal mixing and morphology., *Phys. Chem. Chem. Phys.*, 15, 11441–11453, doi:10.1039/c3cp51595h, 2013.
- Shiraiwa, M., Ueda, K., Pozzer, A., Lammel, G., Kampf, C. J., Fushimi, A., Enami, S., Arangio, A. M., Fröhlich-Nowoisky, J., Fujitani, Y., Furuyama, A., Lakey, P. S. J., Lelieveld, J., Lucas, K., Morino, Y., Pöschl, U., Takahama, S., Takami, A., Tong, H., Weber, B., Yoshino, A. and Sato, K.: Aerosol health effects from molecular to global scales, *Environ. Sci. Technol.*, 51, 13545–13567, doi:10.1021/acs.est.7b04417, 2017.
- Song, M., Marcolli, C., Krieger, U. K., Zuend, A. and Peter, T.: Liquid-liquid phase separation and morphology of internally mixed dicarboxylic acids/ammonium sulfate/water particles, *Atmos. Chem. Phys.*, 12, 2691–2712, doi:10.5194/acp-12-2691-2012, 2012a.
- Song, M., Marcolli, C., Krieger, U. K., Zuend, A. and Peter, T.: Liquid-liquid phase separation in aerosol particles: Dependence on O:C, organic functionalities, and compositional complexity, *Geophys. Res. Lett.*, 39, L19801, doi:10.1029/2012GL052807, 2012b.
- Song, M. J., Marcolli, C., Krieger, U. K., Lienhard, D. M., and Peter, T.: Morphologies of mixed organic/inorganic/aqueous aerosol droplets, *Faraday Discuss.*, 165, 289–316, <https://doi.10.1039/C3fd00049d>, 2013
- Song, M., Liu, P., Martin, S. T. and Bertram, A. K.: Liquid-liquid phase separation in particles containing secondary organic material free of inorganic salts, *Atmos. Chem. Phys.*, 17, 11261–11271, doi:10.5194/acp-17-11261-2017, 2017.



- Song, M., Ham, S., Andrews, R. J., You, Y. and Bertram, A. K.: Liquid-liquid phase separation in organic particles containing one and two organic species: importance of the average O:C, *Atmos. Chem. Phys.*, doi:10.5194/acp-18-12075-2018, 2018.
- 455 Veghte, D. P., Bittner, D. R. and Freedman, M. A.: Cryo-transmission electron microscopy imaging of the morphology of submicrometer aerosol containing organic acids and ammonium sulfate, *Anal. Chem.*, 86(5), 2436–2442, doi:10.1021/ac403279f, 2014.
- Winston, P. W. and Bates, D. H.: Saturated solutions for the control of humidity in biological research, *Ecology*, 41(1), 232–237, 1960.
- 460 Xiaohong, L. and Jian, W.: How important is organic aerosol hygroscopicity to aerosol indirect forcing?, *Environ. Res. Lett.*, 5(4), 44010, doi:10.1088/1748-9326/5/4/044010, 2010.
- You, Y., Renbaum-Wolff, L. and Bertram, A. K.: Liquid-liquid phase separation in particles containing organics mixed with ammonium sulfate, ammonium bisulfate, ammonium nitrate or sodium chloride, *Atmos. Chem. Phys.*, 13, 11723–11734, doi:10.5194/acp-13-11723-2013, 2013.
- 465 You, Y., Smith, M. L., Song, M., Martin, S. T. and Bertram, A. K.: Liquid-liquid phase separation in atmospherically relevant particles consisting of organic species and inorganic salts, *Int. Rev. Phys. Chem.*, 33(1), 43–77, doi:10.1080/0144235X.2014.890786, 2014.
- Zhang, Q., Jimenez, J. L., Canagaratna, M. R., Allan, J. D., Coe, H., Ulbrich, I., Alfarra, M. R., Takami, A., Middlebrook, A. M., Sun, Y. L., Dzepina, K., Dunlea, E., Docherty, K., DeCarlo, P. F., Salcedo, D., Onasch, T., Jayne, J. T., Miyoshi, T., Shimojo, A., Hatakeyama, S., Takegawa, N., Kondo, Y., Schneider, J., Drewnick, F., Borrmann, S., Weimer, S., Demerjian, K., Williams, P., Bower, K., Bahreini, R., Cottrell, L., Griffin, R. J., Rautiainen, J., Sun, J. Y., Zhang, Y. M. and Worsnop, D. R.: Ubiquity and dominance of oxygenated species in organic aerosols in anthropogenically-influenced Northern Hemisphere midlatitudes, *Geophys. Res. Lett.*, 34(13), 1–6, doi:10.1029/2007GL029979, 2007.
- 475 Zuend, A. and Seinfeld, J. H.: Modeling the gas-particle partitioning of secondary organic aerosol: The importance of liquid-liquid phase separation, *Atmos. Chem. Phys.*, 12, 3857–3882, doi:10.5194/acp-12-3857-2012, 2012.



- 480 Zuend, A., Marcolli, C., Peter, T. and Seinfeld, J. H.: Computation of liquid-liquid equilibria and phase stabilities: Implications for RH-dependent gas/particle partitioning of organic-inorganic aerosols, *Atmos. Chem. Phys.*, 10(16), 7795–7820, doi:10.5194/acp-10-7795-2010, 2010.